# 1. Iron Oxides as dehydrogenation catalysts (Surface Structure)

## 1.1 Introduction

The metal oxides represent a family of materials with remarkable diversity of properties which make them of great technological and scientific importance. Among the many fields in which metal oxides are applied, catalysis science attracts a great interest and importance in our everyday life. Metal oxides are not only used as catalyst support for many processes e.g. $Al_2O_3$ and MgO, but also and more important, they are themselves catalysts for many important reactions including oxidation reactions, selective oxidation and reduction reactions.

Dehydrogenation of ethylbenzene (EB) is one of those reactions catalyzed by standard dehydrogenation metal oxide catalysts, such as CaO, $Al_2O_3$, $Cr_2O_3/Al_2O_3$, $V_2O_3$, $MoO_3/Al_2O_3$ and $Fe_2O_3$[1]. In the presence of steam it was found that the intrinsic activities of the different un-promoted metal oxides do not differ greatly, however, the activity of alkali promoted iron oxide catalyst is about one order of magnitude higher than that of the un-promoted iron oxide[1].

Among various alkali and alkaline earth promoters, Cs, Rb and K have proven to show the best performance. Being cheaper than both Cs and Rb, potassium is the preferred promoter. This system was thus widely studied and commercially applied[1,2]. The technical catalyst is composed of unsupported Fe-K double oxide system and it was suggested that the active catalytic phase is $KFeO_2$[3].

Systematic investigation of the catalytic properties of this system was achieved by studying heteroepitaxially grown films[4-6]. Bulk and surface structure of different iron oxide and K-promoted iron oxide phases were particularly investigated. And in the aim to elucidate the reaction mechanism, and to identify the active sites, surface termination was of great interest. It also enables performing active model catalyst modelling and developing procedures which simulate the catalytic reaction.

Previously, Dynamical Low Energy Electron Diffraction calculations (LEED-IV) and Ion Scattering Spectroscopy (ISS) were used in the investigation of surface

termination of different iron oxide phases. FeO(111) was found to be oxygen-terminated[7], $Fe_2O_3$(0001) was found to be preparation-dependent. It exhibits either oxygen termination or most likely hydroxyl termination according to preparation conditions[8]. $Fe_3O_4$, on the other hand, was found to be iron-terminated[7,9].
Herein the investigation is expanded and the termination of the potassium promoted phase is explored using ISS. The influence of changing the incidence angle on the ISS spectrum of a K-promoted iron oxide thin film over Pt(111) substrate is followed and analyzed.

## 1.2 Experimental details and methodology

### 1.2.1 Preparation of iron oxide films

Iron oxide films were prepared as described in ref. 7 by deposition of iron at room temperature over a Pt(111) substrate followed by subsequent oxidation at temperatures in the range of 600 $^{o}$C to 750 $^{o}$C in ~ $1x10^{-6}$ mbar partial pressure of oxygen.

Pt (111) was cleaned by repeated sputter-anneal/oxidation cycles. The cleanliness of the Pt surface was confirmed by its characteristic sharp LEED pattern and ISS spectra.

FeO was prepared by depositing 1-2 monolayers of iron over Pt(111) substrate followed by oxidation of the film at a temperature of 600 $^{o}$C in an $O_2$ partial pressure of $1x10^{-6}$ mbar.

$Fe_3O_4$ was prepared by repeatedly depositing 2-3 monolayers of iron and oxidizing them at a temperature of 650-700 $^{o}$C in an oxygen partial pressure of $1x10^{-6}$ mbar. A total of about 10 monolayers of iron are needed to obtain a closed $Fe_3O_4$ film.

K-promoted phases are prepared by subsequently depositing potassium on an $Fe_3O_4$ film followed by oxidation at a temperature of 650 $^{o}$C in an oxygen partial pressure of about $1x10^{-6}$mbar.

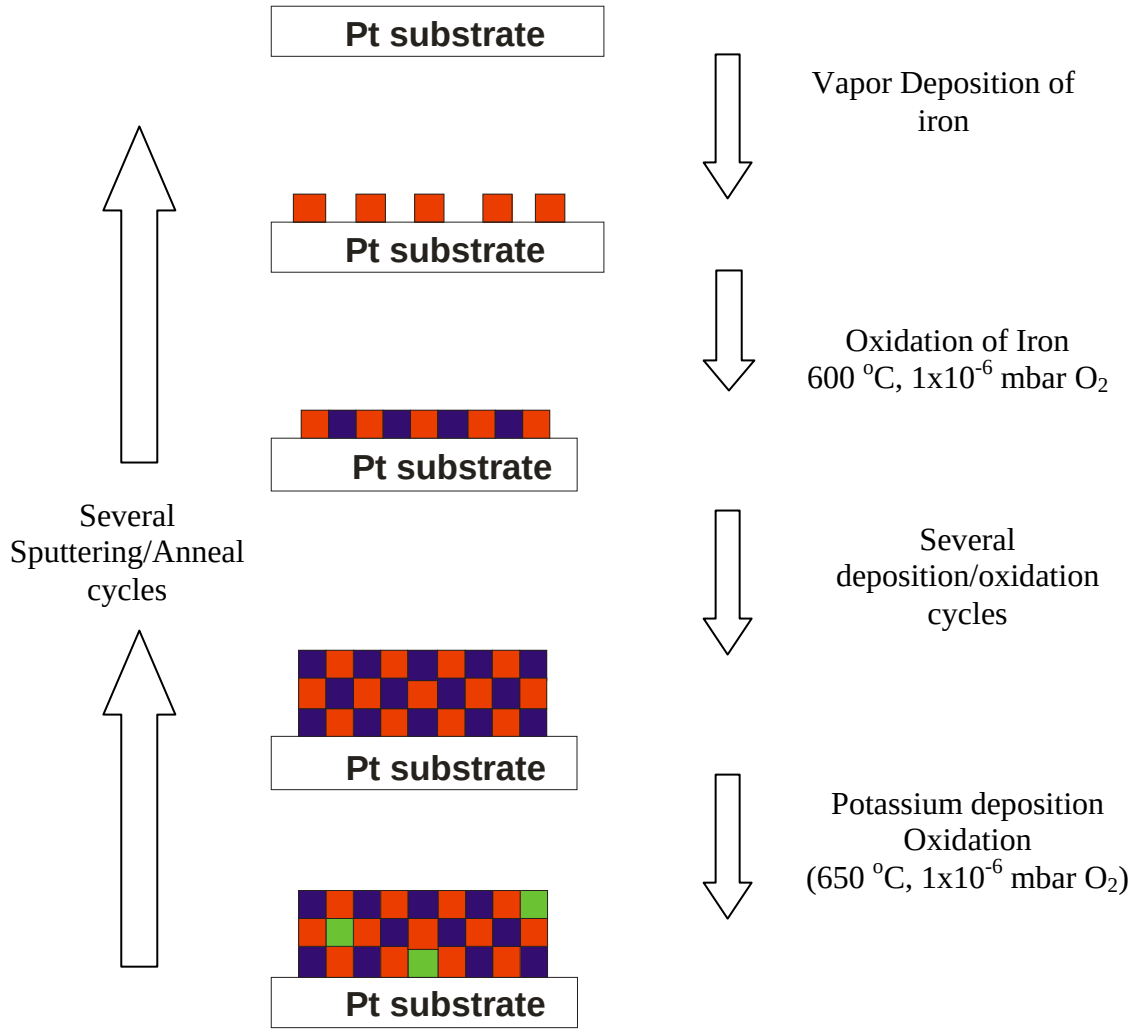


Figure 1.1. Preparation of Iron oxide films

### 1.2.2 Flux Calibration of the iron source

Flux calibration of the iron source was performed using ISS. Iron was deposited on a Pt(111) substrate in small doses while monitoring the signal of Pt. The amount of iron needed (deposition time at constant rate) before the Pt signal disappeared, was assumed to represent a monolayer. It was not possible to combine LEED measurements to this procedure because the sample should be annealed before LEED can be used. Annealing causes iron to migrate deeply in the Pt substrate forming an iron/platinum alloy.

### 1.2.3 Analysis methods

#### 1.2.3.1 Low Energy Electron Diffraction (LEED)

This technique uses diffraction effects. The surface crystallographic structure is determined by bombarding the surface with low energy electrons (approx. 10-200 eV) and observing diffracted electrons as spots on a phosphorescent screen. The relative position of the spots on the screen shows the surface crystallographic structure.

The diffraction patterns were recorded with a CCD camera from the LEED screen

#### 1.2.3.2 Ion Scattering Spectroscopy (ISS)

Basic concept:
Ion Scattering Spectroscopy (ISS) is one of the most surface sensitive spectroscopic techniques[10]. In this technique an approximately monoenergetic beam of ions in the energy range of 0.5 – 3.0 k eV is directed to the surface in some well-defined direction and the energy of the primary scattered ions is measured at a well-defined emission direction. This scattering process is almost exactly described by simple free atom two-body collision and can easily be analysed on the basis of energy and momentum conservation. This is described in equation 1.1

$$\frac{E_1}{E_0} = \frac{1}{(1+A)^2}\left[\cos\theta_1 + \left(A^2 - \sin^2\theta_1\right)^{\frac{1}{2}}\right]^2 \qquad A = \frac{M_2}{M_1} > 1 \qquad (1.1)$$

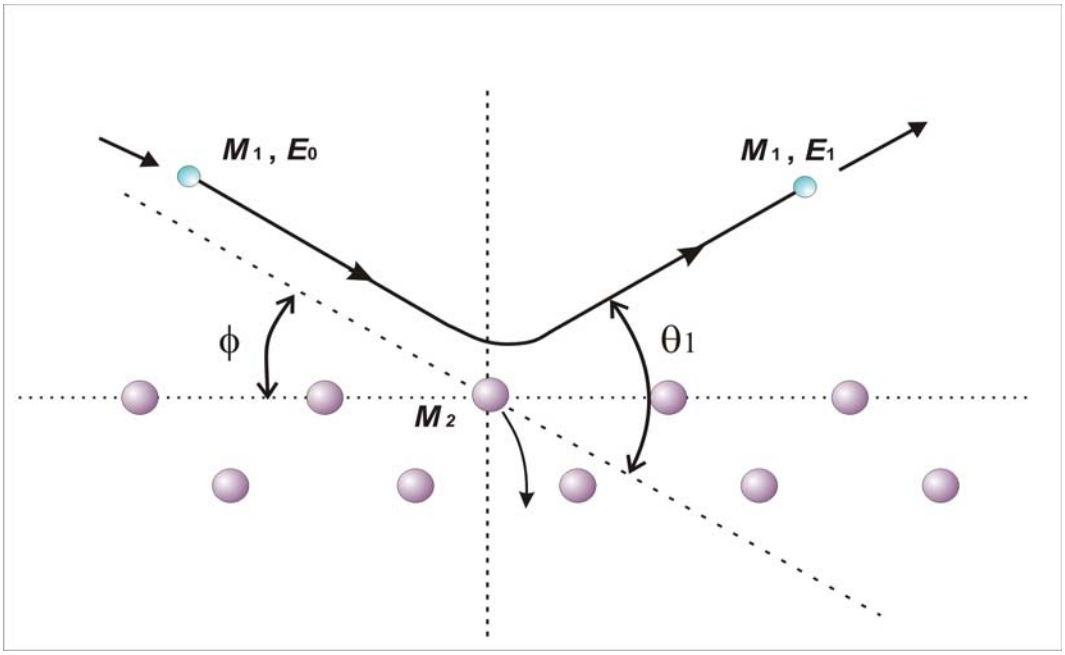

Figure 1.2. Principle of Ion Scattering Spectroscopy

Where *Eo* is the initial energy, $E_1$ is the energy of the scattered ions, $\theta_1$ is the scattering angle, $M_1$ and $M_2$ are the ion and target atom masses, respectively. This equation directly relates the energy of the scattered particle to the mass of the target.

To perform the ISS measurements, an ion gun from Omicron was used in cooperation with a Focus cylindrical sector analyser mounted normal to the sample surface. In all the discussed measurements, following parameters were used:
Energy of incident He ions: 500 eV
He pressure: $1x10^{-6}$ mbar

### 1.3 Results and Discussion

Figure 1.3 shows the ISS spectrum of FeO and $Fe_3O_4$ films over Pt(111), the absence of platinum peak confirms the full coverage of the surface by the iron oxide film. The oxygen peak appears at ~ 213 eV while that of iron at 375 eV. These positions are lower than the calculated positions ($E_1$) in equation 1.1 (232 eV and 403 eV for oxygen and iron, respectively). This energy loss is due to inelastic effects encountered in the scattering process[11]. These inelastic processes include the fact that the target atom is not free but bound to surrounding atoms, the possibility that the target atom be electronically excited and the inelastic electron exchange between

the projectile ion and the surface. Thus, the energies calculated in 1.1 roughly correspond to the high-energy "foot" of the peak.

No direct quantitative information can be deduced from these spectra because the peak intensity corresponding to any element in ISS is influenced by several factors including scattering cross section, neutralization and re-ionization probability in addition to its concentration on the surface[12].

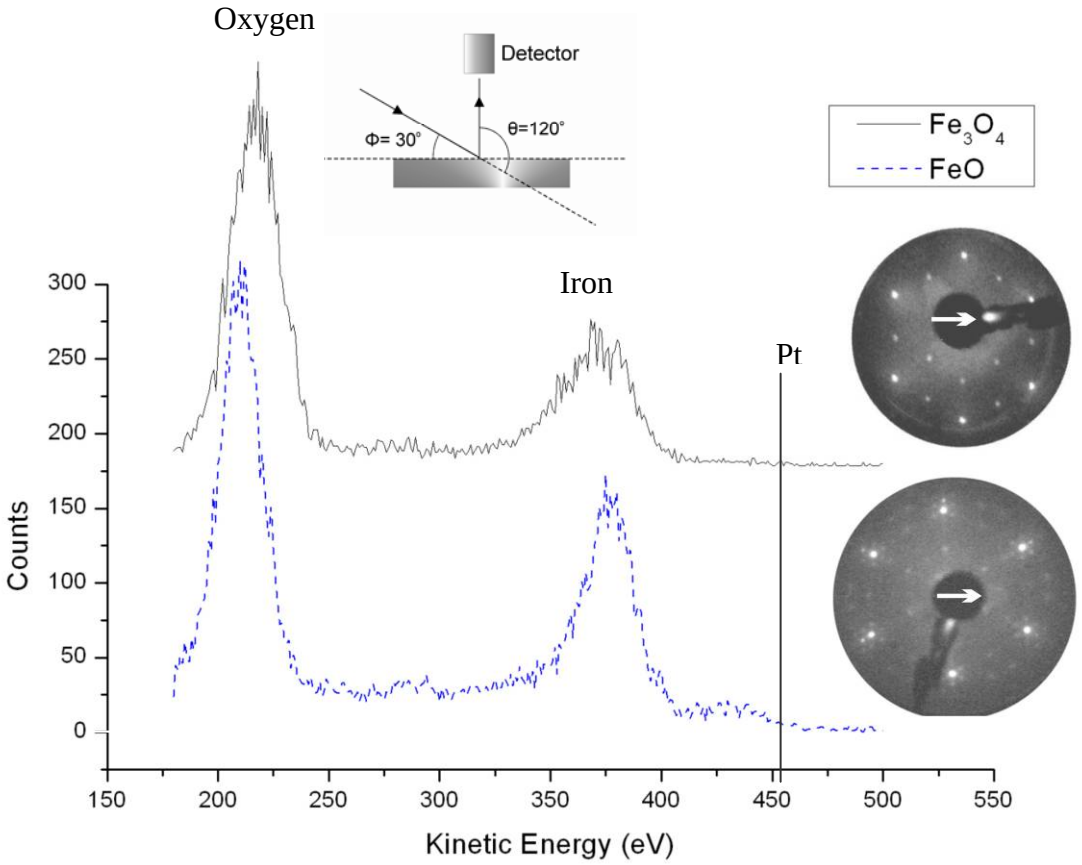


Figure1.3. ISS Spectra of FeO and $Fe_3O_4$ films over Pt(111)
*The arrows in the LEED patterns show the azimuthal direction of ISS experiments*

In figure 1.4, the ISS spectrum of the K-promoted iron oxide phase is shown. The peak of iron which should appear at 375 eV (Th. 403 eV) appears as a shoulder on the high energy side of the broad peak of potassium having its maximum at 340 eV (Th. 367 eV). Between the peaks of iron and potassium, a shoulder appears at about 358 eV. This can be caused by double scattering or re-ionization process[10,11]. As

mentioned above, no direct quantitative or structural information can be deduced from this single spectrum.

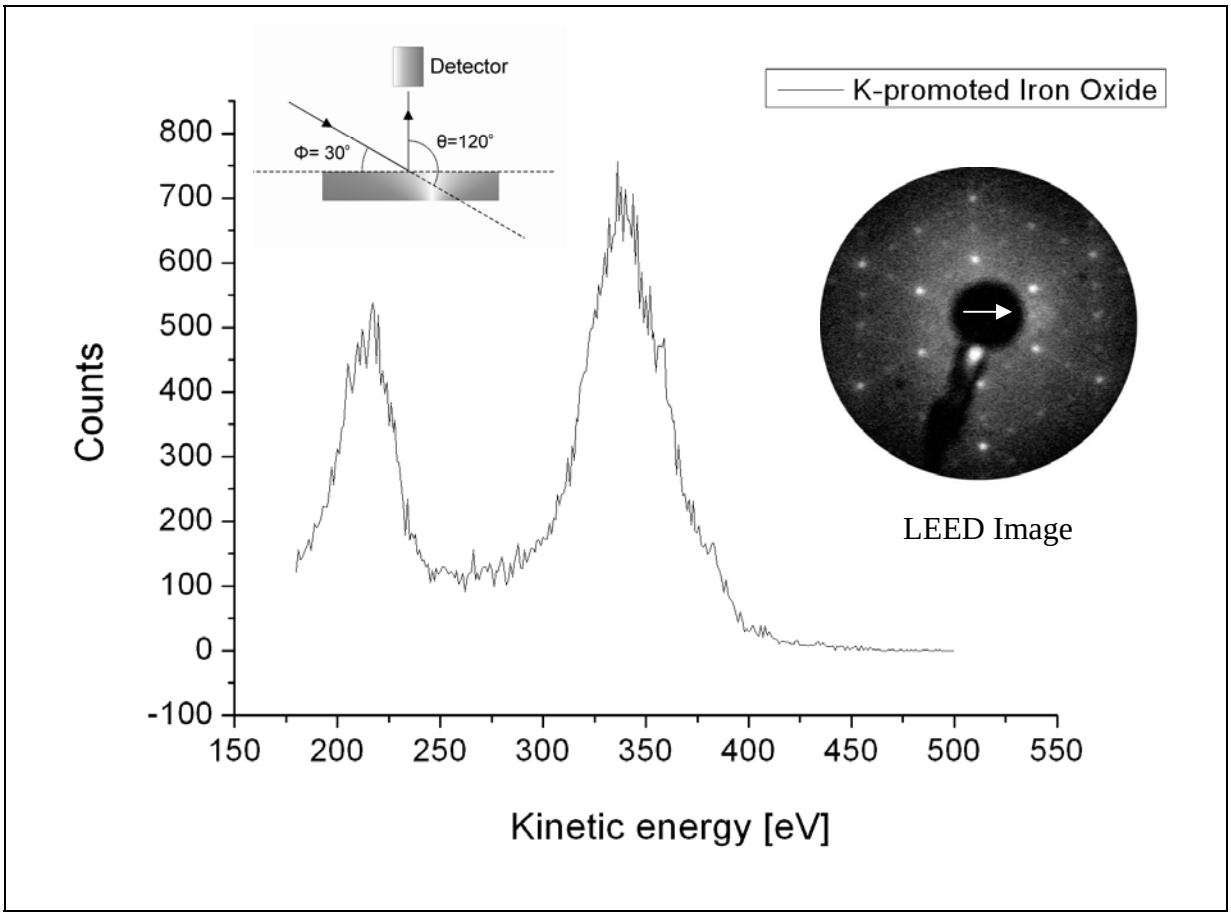


Figure 1.4 ISS spectrum of the K-promoted iron oxide
*The arrow in the LEED patterns shows the azimuthal direction of ISS experiments*

By rotating the sample, the spectra of this phase were recorded at different incident angle values (figure 1.6) keeping the scattering angle constant. As expected, changing the incidence angle influences the spectra. Hence, starting from an incidence angle of 37.5$^{o}$, and upon decreasing the incidence angle, the intensity of all peaks decreases, This is mainly due to the fact that the incident ion beam spreads on a larger surface area at lower incidence angle decreasing the ion flux per unit area. This is shown in fig. 1.5. In the case of beam (1) with an incidence angle of 30$^{o}$, the ion beam bombards the surface area (a). In the case of ion beam (2) which has the same ion flux as beam (1), but with an incidence angle of 15$^{o}$, the ion beam bombards the surface area (b). It is clear that in the second case the bombarded area is larger than that in the first case while the detected area is the same in both

cases. This decreases the number of scattered ions that can be detected. Another possible reason for decreasing the peak intensity at lower incidence angles is the increasing possibility for double scattering -although not very probable for He ions- and neutralization of incident ions at lower incidence angles.

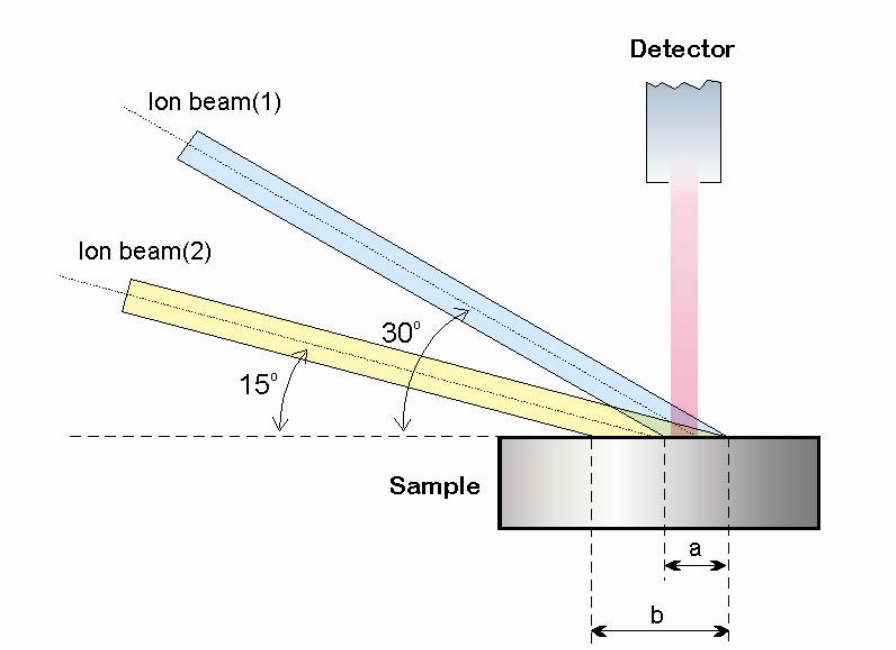


Figure 1.5 Effect of changing the incidence angle on ion beam in ISS

The iron component appears as a shoulder on the high energy side of the potassium peak. It diminishes and disappears at an incidence angle of ~20$^{o}$ and lower. On the other hand, it can be also seen that the intensity of oxygen peak decreases faster than that of potassium, this is clearly seen in figure 1.7 in which the ratio of peak height of oxygen to that of potassium is plotted versus the incidence angle. In order to understand this, shadowing effect in ISS must be considered.

When describing the interaction of an incident ion scattering from an atom with a defined screening length, and drawing a set of ion trajectories, one ends with what is called a shadow cone behind the scatterer atom (figure 1.8). Atoms in this cone are practically not seen by the incident ions and these atoms will not contribute to the scattering process. This is shown in figure (1.9). In this figure, the top atomic layer is composed of atoms of (type A). It is clear that these atoms will shadow much (if not all) of the second atom layer (type B) depending on the direction of trajectory ions and azimuthal angle. Decreasing the incidence angle would result in shadowing

more and more of the second atom layer. On the other hand, increasing of the incidence angle would have the opposite effect and the second atomic layer would contribute more to the scattering process.

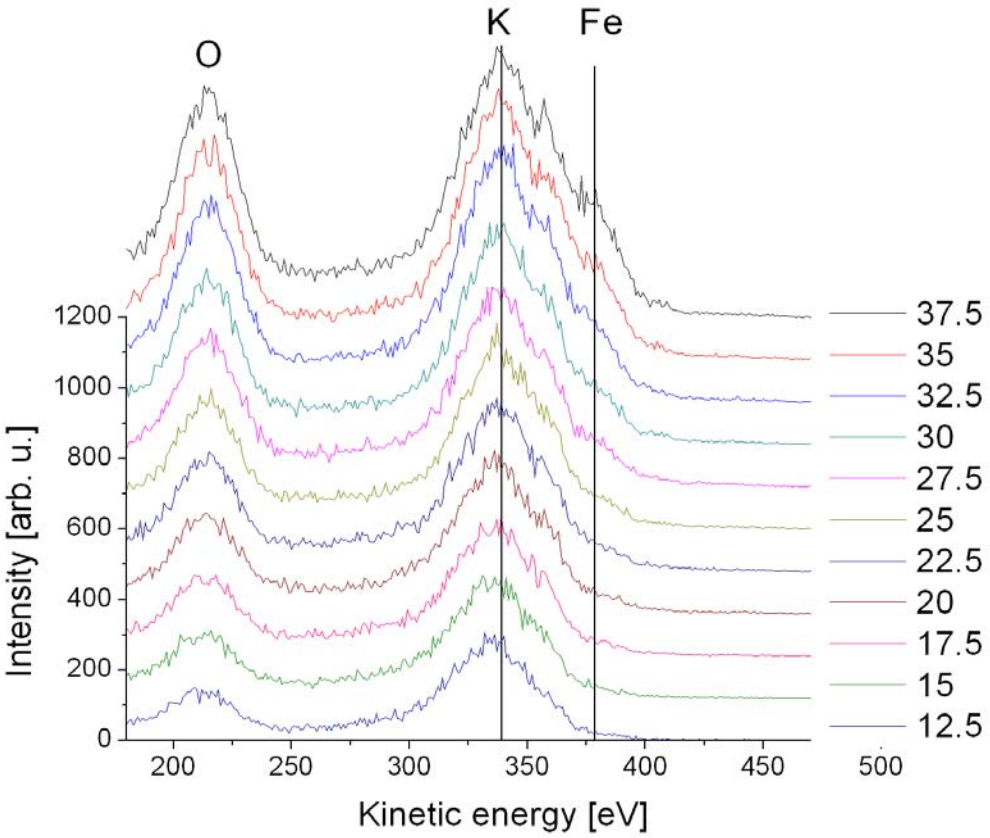


Figure 1.6 ISS Spectra of K-promoted iron oxide films at different incidence angle

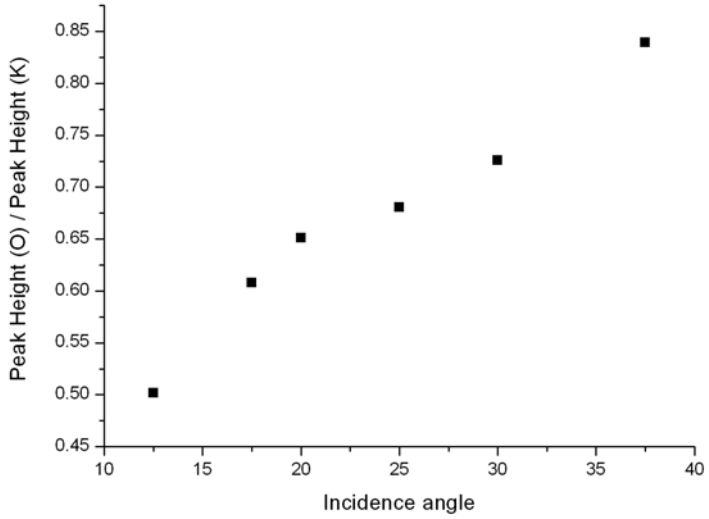


Figure 1.7 Effect of changing the incidence angle on the ratio between peak height of oxygen to that of potassium in ISS measurements.

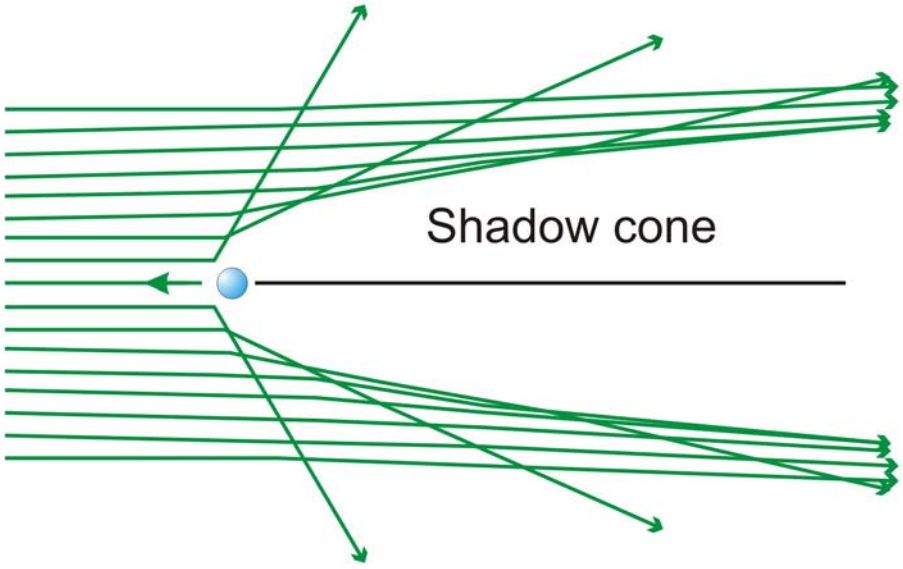


Figure 1.8 Shadow cone of scattering trajectories.

Now, applying that on the ISS spectra of the potassium promoted iron oxide film in figure 1.6, we can interpret the disappearance of the iron signal at lower incidence angles as a result of iron atoms lying in a deeper, e.g. the third atom layer below potassium and oxygen. As well, the signal of oxygen diminishes faster than that of potassium which implies that oxygen lies below potassium. This suggests a surface

structure (figure 1.10) terminated by potassium atoms followed by oxygen atoms in the second atom layer and iron in the third atom layer. This result confirms previous models and structure studies on this phase[13].

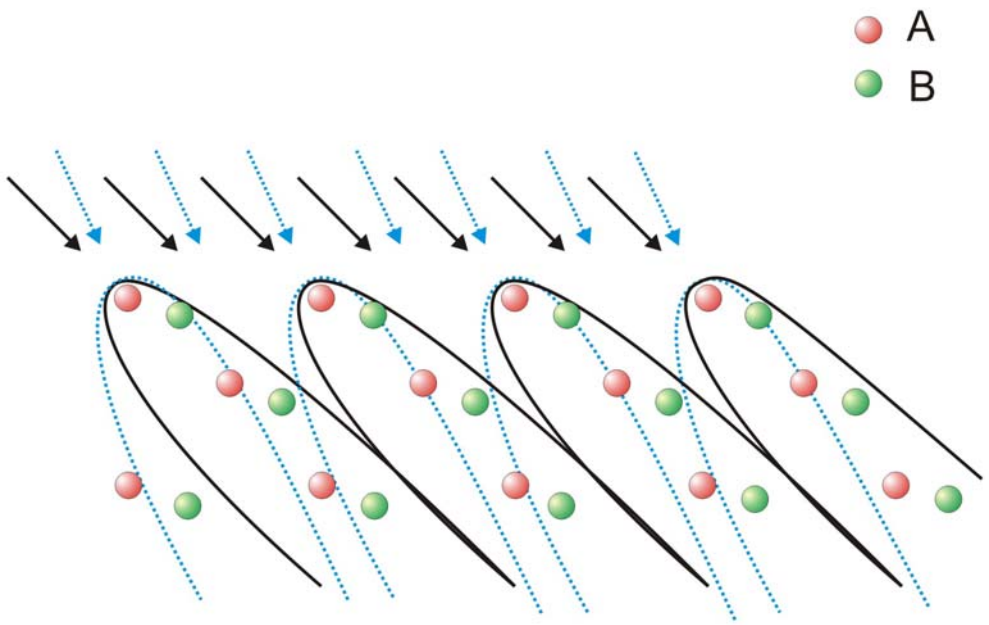


Figure 1.9. Shadowing effect in ISS spectroscopy at different incidence angles

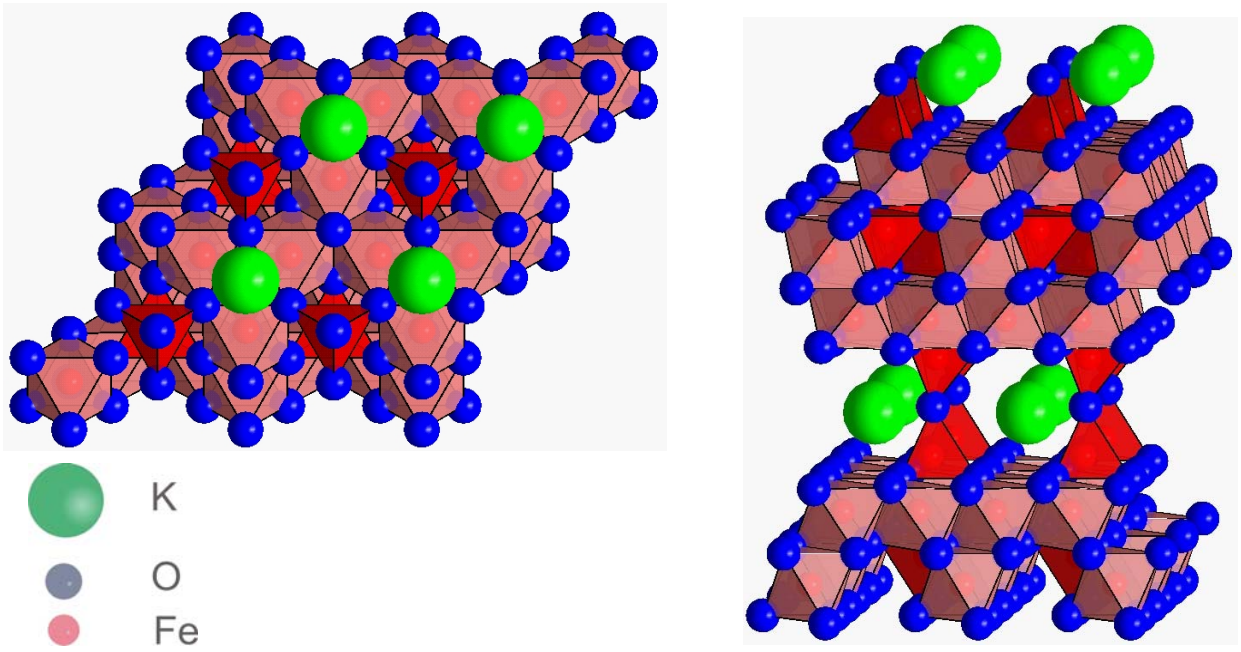


a b

Figure 1.10. Structure model of the K-promoted iron oxide film. (a) Top view, (b) side view

## 1.4 Conclusion

It was shown that the K-promoted (2x2) phase has a potassium and oxygen terminated surface structure. This confirms the models Proposed previously in our laboratories. So, the only iron terminated surface structure is that of $Fe_3O_4$, which is the phase with the lowest catalytic activity among the iron oxide phases studied in our laboratories. This states that iron is needed in the catalyst but not on the topmost atomic layer, otherwise it binds strongly to both the reactants and the products and hinders the catalytic process. This result also agrees with the previous studies stating that potassium as a promoter should be on the surface of the catalyst to have its promoting action[1].

Talking again about the industrial application of this catalytic system, it should be stated that this process needs large amounts of superheated steam. This steam has the advantage of preventing the thermal cracking of ethylbenzene at these high temperatures, removing the carbonaceous residues, and shifting the equilibrium towards higher styrene concentrations. But, it plays a role in catalyst deactivation as well because it causes potassium migration in the form of KOH towards the reactor outlet. Potassium also migrates by the action of temperature towards the center of catalyst pellets which is colder than the surface. This two-directional potassium migration is another reason for deactivation in addition to the previously-mentioned coking problem.

These and other reasons caused the researchers to think about other approaches to achieve the conversion of ethyl benzene to styrene at better economical conditions. Several systems and processes were suggested and investigated by the scientific community. Among these, oxidative dehydrogenation -which is the key subject of the rest of this work- proved to be a promising candidate with various advantages over the conventional dehydrogenation process.

(1) Lee, E. H. *Catal. Revs.* **1974**, *8*, 285 - 305.
(2) Muhler, M.; Schlögl, R.; Ertl, G. *Journal of Catalysis* **1992**, *138*, 413-444.
(3) Muhler, M.; Schutze, J.; Wesemann, M.; Rayment, T.; Dent, A.; Schlögl, R.; Ertl, G. *Journal of Catalysis* **1990**, *126*, 339-360.

(4) Kuhrs, C.; Arita, Y.; Weiss, W.; Ranke, W.; Schlögl, R. *Topics in Catalysis* **2001**, *14*, 111-123.
(5) Street, S. C.; Xu, C.; Goodman, D. W. *Annual Review of Physical Chemistry* **1997**, *48*, 43-68.
(6) Weiss, W.; Schlögl, R. *Topics in Catalysis* **2000**, *13*, 75-90.
(7) Weiss, W.; Ranke, W. *Progress in Surface Science* **2002**, *70*, 1-151.
(8) Ketteler, G.; Weiss, W.; Ranke, W. *Surface Review and Letters* **2001**, *8*, 661-683.
(9) Lemire, C.; Meyer, R.; Henrich, V. E.; Shaikhutdinov, S.; Freund, H. J. *Surface Science* **2004**, *572*, 103-114.
(10) Niehus, H.; Heiland, W.; Taglauer, E. *Surface Science Reports* **1993**, *17*, 213-303.
(11) Aono, M.; Souda, R. *Nuclear Instruments and Methods in Physics Research Section B: Beam Interactions with Materials and Atoms* **1987**, *27*, 55-64.
(12) Taglauer, E.; Heiland, W. *Applied Physics A: Materials Science & Processing* **1976**, *9*, 261-275.
(13) Joseph, Y.; Ketteler, G.; Kuhrs, C.; Ranke, W.; Weiss, W.; Schlögl, R. *Physical Chemistry Chemical Physics* **2001**, *3*, 4141-4153.